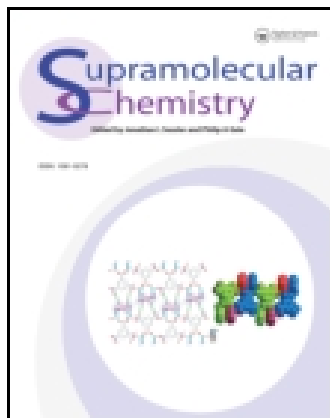


This article was downloaded by: [North Dakota State University]

On: 09 October 2014, At: 17:08

Publisher: Taylor & Francis

Informa Ltd Registered in England and Wales Registered Number: 1072954 Registered office: Mortimer House, 37-41 Mortimer Street, London W1T 3JH, UK



## Supramolecular Chemistry

Publication details, including instructions for authors and subscription information:

<http://www.tandfonline.com/loi/gsch20>

### A silver-induced metal-organic gel based on biscalboxyl-functionalised benzimidazole derivative: stimuli responsive and dye sorption

You-Ming Zhang<sup>a</sup>, Xing-Mei You<sup>a</sup>, Hong Yao<sup>a</sup>, Ying Guo<sup>a</sup>, Peng Zhang<sup>a</sup>, Bing-Bing Shi<sup>a</sup>, Jun Liu<sup>a</sup>, Qi Lin<sup>a</sup> & Tai-Bao Wei<sup>a</sup>

<sup>a</sup> Key Laboratory of Eco-Environment-Related Polymer Materials of Ministry of Education, Gansu Key Laboratory of Polymer Materials, College of Chemistry and Chemical Engineering, Northwest Normal University, Lanzhou, 730070, China

Published online: 21 Aug 2013.



[Click for updates](#)

To cite this article: You-Ming Zhang, Xing-Mei You, Hong Yao, Ying Guo, Peng Zhang, Bing-Bing Shi, Jun Liu, Qi Lin & Tai-Bao Wei (2014) A silver-induced metal-organic gel based on biscalboxyl-functionalised benzimidazole derivative: stimuli responsive and dye sorption, *Supramolecular Chemistry*, 26:1, 39-47, DOI: [10.1080/10610278.2013.822968](https://doi.org/10.1080/10610278.2013.822968)

To link to this article: <http://dx.doi.org/10.1080/10610278.2013.822968>

PLEASE SCROLL DOWN FOR ARTICLE

Taylor & Francis makes every effort to ensure the accuracy of all the information (the "Content") contained in the publications on our platform. However, Taylor & Francis, our agents, and our licensors make no representations or warranties whatsoever as to the accuracy, completeness, or suitability for any purpose of the Content. Any opinions and views expressed in this publication are the opinions and views of the authors, and are not the views of or endorsed by Taylor & Francis. The accuracy of the Content should not be relied upon and should be independently verified with primary sources of information. Taylor and Francis shall not be liable for any losses, actions, claims, proceedings, demands, costs, expenses, damages, and other liabilities whatsoever or howsoever caused arising directly or indirectly in connection with, in relation to or arising out of the use of the Content.

This article may be used for research, teaching, and private study purposes. Any substantial or systematic reproduction, redistribution, reselling, loan, sub-licensing, systematic supply, or distribution in any form to anyone is expressly forbidden. Terms & Conditions of access and use can be found at <http://www.tandfonline.com/page/terms-and-conditions>

## A silver-induced metal-organic gel based on biscarboxyl-functionalised benzimidazole derivative: stimuli responsive and dye sorption

You-Ming Zhang, Xing-Mei You, Hong Yao, Ying Guo, Peng Zhang, Bing-Bing Shi, Jun Liu, Qi Lin and Tai-Bao Wei\*

Key Laboratory of Eco-Environment-Related Polymer Materials of Ministry of Education, Gansu Key Laboratory of Polymer Materials, College of Chemistry and Chemical Engineering, Northwest Normal University, Lanzhou 730070, China

(Received 12 January 2013; final version received 25 June 2013)

A multi-responsiveness supramolecular metal-organic gel (MOG) has been prepared by using silver (I) nitrate and a simple ligand (L17) based on a biscarboxyl-functionalised benzimidazole derivative. The MOG that displays the formation of well-developed nanofibrillar networks composed of intertwined fibres was characterised by using field emission scanning electron microscopy (FESEM), Fourier transform infrared (FT-IR) spectroscopy and powder X-ray diffraction (XRD) techniques. The FT-IR spectra and XRD show that supramolecular MOG was formed through an effective coordination of the ligand and  $\text{Ag}^+$ . This MOG reveals outstanding reversible sol–gel transitions induced by changes of temperature and pH, as well as by addition of  $\text{NH}_4\text{OH}$ , ethylene diamine tetraacetic acid and  $\text{Na}_2\text{S}$ . In addition, the MOG also shows a good ability in dye sorption. These results demonstrate that this multichannel responsive smart MOG has the potential to be widely applied in materials science.

**Keywords:** supramolecular metal-organic gel; benzimidazole derivative; reversible change; stimuli responsive; dye sorption

### 1. Introduction

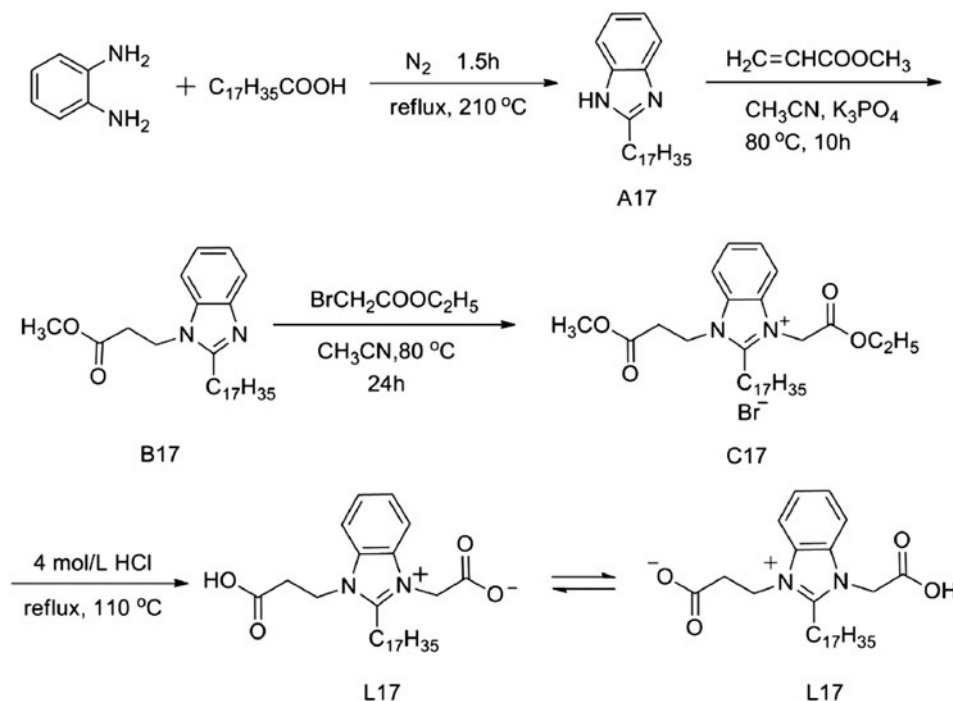
Low molecular weight organogels (LMWGs) represent an important type of soft materials, in which the organic or aqueous phase is immobilised in a nanofibrillar network formed from self-assembled nanostructures of gelator molecules (1, 2). The non-covalent interactions, such as hydrogen bonding,  $\pi$ – $\pi$  stacking, hydrophobic interactions and van der Waals interactions, play an important role in self-assembling LMWGs to form entangled nanostructures (3, 4). Recently, LMWGs have received more attention than their polymeric analogues for a large amount of scientific applications, such as food (5), tissue engineering (6), pollutant capture and removal (7), optical devices, drug delivery vehicles (8, 9) and so on. In spite of supramolecular organogels or hydrogels using molecules containing diverse functional groups, which have been well researched (2–4, 10, 11), metal-organic gels (MOGs) or metallogels based on metal coordination bonds have also been concerned by Rowan et al. (12, 13). In general, metal–ligand coordination is used to enhance the intermolecular interactions. In addition, ligand molecules that initially could not form gels must be gelled by the addition of metal ions (14). Nowadays, there have been reported organogels and metallogels that are responsive to ultrasound (15–18), mechanical stimulation (19), sound (20, 21), metallic cations (22), temperature (23), anions

(24, 25) and light (26, 27); however, only a few reports currently exist on controllable gelation systems based on reversible changes in metallogels induced by pH,  $\text{Na}_2\text{S}$  and ethylene diamine tetraacetic acid (EDTA) (28).

Recently, it has been explored that the molecules including pyridyl bis (urea), terpyridyl or bis (benzimidazole). Show good properties in gelating with metal ions (29–31). For instance, the terpyridyl-based ligands have been effectively shown to form gels with platinum salts and their photophysical properties were investigated. The pyridyl bis (urea)-based ligand has been shown to form a shear-induced MOG with  $\text{Cu(II)}$  bromide salt (24). Recently, the catalytic activity of imidazole-based gels has also been researched (32). In very few cases, dye sorption (13, 33) phenomena have also been studied with the gel materials. Among all the above-mentioned MOGs, the N-containing unit of the gelator molecule plays an important role in the formation of gel. To date, a few examples of biscarboxyl-functionalised benzimidazole derivatives as gelators have been reported (34, 35).

In this paper, we designed and synthesised a biscarboxyl-functionalised benzimidazole derivative with a simple structure (Scheme 1) on the basis of our previous work (34–36). As a result, the experiments showed that ligand L17 as an LMW gelator could be induced to form MOG with selectivity for  $\text{Ag(I)}$ . The L17 MOG also revealed a

\*Corresponding author. Email: [weitaobao@126.com](mailto:weitaobao@126.com)



Scheme 1. Synthesis of Gelator L17.

reversible sol–gel transition induced by the changes of temperature, pH,  $\text{NH}_4\text{OH}$ , EDTA and  $\text{Na}_2\text{S}$ . Moreover, it can also be used in dye sorption (methyl orange). We believe that the multichannel responsive smart silver (I) nitrate MOG of L17 has the potential to be widely applied in materials science.

## 2. Experimental

### 2.1 General experimental section

Melting points were measured on an X-4 digital melting point apparatus (uncorrected).  $^1\text{H}$  NMR spectra were recorded with a Mercury-400BB spectrometer (VARIAN, USA, <http://www.varian.com>) at 400 MHz, with tetramethylsilane as an internal standard. NMR spectra were referenced to the solvent. The infrared spectra were recorded on a Digilab FTS-3000 Fourier transform infrared (FT-IR) spectrophotometer (Digilab Inc, USA, <http://210028.us.all.biz>). Mass spectra were recorded on an esquire 6000 MS instrument (Bruker Daltonics Inc, <http://www.bruker.com>) equipped with an electrospray (ESI) ion source with version 3.4 of Bruker Daltonics Data Analysis (Bruker Daltonics Inc, [http://www.gongchang.com/Bruker\\_Daltonics\\_Inc-company](http://www.gongchang.com/Bruker_Daltonics_Inc-company)) as the data collection system. The 1:1 xerogel of MOG was coated on a glass plate and the solvent was slowly evaporated. The glass plates with dry gels were then fixed on a sample holder and subjected to X-ray diffraction (XRD) analysis at room temperature on a Japan Rigaku D/MAX-2400/PC

diffractometer (Japan Rigaku, <http://www.rigaku.com>). XRD patterns were recorded at a scanning rate of  $5^\circ$  per minute in the  $2\theta$  range of  $2\text{--}50^\circ$  with  $\text{Cu K}\alpha$  radiation. The morphologies and sizes of the xerogels were characterised using field emission scanning electron microscopy (FESEM, JSM-6701F) at an accelerating voltage of 8 kV. All reagents of analytical grade were purchased from Alfa Aesar.

### 2.2 Synthesis of compound L17

The synthesis of 2-heptadecylbenzimidazole (A17) was accomplished on the basis of previous work (37). 2-Heptadecylbenzimidazole (6.88 g, 20 mmol), methyl acrylate (2.07 g, 24 mmol) and a catalytic amount of  $\text{K}_3\text{PO}_4$  (1.33 g, 5 mmol) were combined in absolute acetonitrile (60 ml). The solution was stirred at  $80^\circ\text{C}$  for 10 h. After cooling to room temperature, the white precipitate was filtered and the filtrate was evaporated (using a rotary evaporator) to obtain a brown oily liquid B17 (4.64 g, 54%). A mixture of compound B17 (4.30 g, 10 mmol) and bromoacetate (2.00 g, 12 mmol) in dry absolute acetonitrile (60 ml) was stirred at  $80^\circ\text{C}$  for 24 h. After cooling to room temperature, the solution was evaporated (using a rotary evaporator) to obtain a damp-dry white solid, and the white solid was evaporated under reduced pressure and washed with absolute acetone several times, after stoving to obtain a dry white powdery product C17 (3.05 g, 50%). After further purification,

Table 1. Gelation properties of MOG.

| Solvent                                   | Gelation behavior | Gelating time | MGC/mg ml <sup>-1</sup> | T <sub>gel</sub> /°C |
|---|-------------------|---------------|-------------------------|----------------------|
| MeOH                                      | G                 | 15 min        | 5.00                    | 18                   |
| MeOH–H <sub>2</sub> O (V/V = 1:1)         | G                 | 10 min        | 1.51                    | 19                   |
| EtOH                                      | S                 | –             | –                       | –                    |
| EtOH–H <sub>2</sub> O (V/V = 1:1)         | G                 | 2 h           | 2.67                    | 28                   |
| nPrOH                                     | S                 | –             | –                       | –                    |
| nPrOH–H <sub>2</sub> O (V/V = 1:1)        | S                 | –             | –                       | –                    |
| iPrOH                                     | G                 | 19 min        | 4.17                    | 33                   |
| iPrOH–H <sub>2</sub> O (V/V = 1:1)        | G                 | 14 min        | 1.57                    | 25                   |
| nBuOH                                     | S                 | –             | –                       | –                    |
| tBuOH                                     | SP                | –             | –                       | –                    |
| iPeOH                                     | SP                | –             | –                       | –                    |
| Cyclohexanol                              | SP                | –             | –                       | –                    |
| Benzene                                   | SP                | –             | –                       | –                    |
| Acetone                                   | SP                | –             | –                       | –                    |
| Acetone–H <sub>2</sub> O (V/V = 1:1)      | G                 | 6 min         | 3.64                    | 16                   |
| Acetonitrile                              | SP                | –             | –                       | –                    |
| Acetonitrile–H <sub>2</sub> O (V/V = 1:1) | G                 | 14 min        | 3.33                    | 18                   |
| DMSO                                      | S                 | –             | –                       | –                    |
| DMF                                       | G                 | 18 min        | 9.52                    | 19                   |
| DMF–H <sub>2</sub> O (V/V = 1:1)          | WG                | ca.1 day      | 4.76                    | 16                   |
| Dichloromethane                           | SP                | –             | –                       | –                    |
| Chloroform                                | SP                | –             | –                       | –                    |
| Carbon tetrachloride                      | SP                | –             | –                       | –                    |

Note: G, gel; WG, weak gel; S, solution; SP, solution precipitate.

compound C17 (6.09 g, 10 mmol) was dissolved in 50 ml of hot HCl (4 mol l<sup>-1</sup>), and the solution was stirred at 110°C for 12 h. The solution was evaporated under reduced pressure, and the residue was recrystallised from EtOH–H<sub>2</sub>O (1:10 V/V) to give the product L17 (2.77 g, 57%). Mp: 203–205°C. <sup>1</sup>H NMR (400 MHz, DMSO d<sub>6</sub>): δ (ppm) 0.85–0.86 (t, 3H), 1.15–1.23 (m, 26H), 1.43 (t, 2H), 1.65 (t, 2H), 2.88–2.90 (t, 2H), 3.25–3.27 (t, 2H), 4.68–4.71 (t, 2H), 4.91 (s, 2H), 7.57–7.58 (m, 2H), 7.82–7.84 (d, 1H), 8.01–8.03 (m, 1H), 12.13 (s, 1H). IR (KBr, cm<sup>-1</sup>): ν 3421, 3055, 2921, 2851, 1726, 1671, 1526, 1470, 1211, 755. ESI-MS: calculated for (L17 + H)<sup>+</sup>487 and found 487.6.

### 3. Results and discussion

#### 3.1 The forming process of the gel

A simple LMW gelator L17 was designed and synthesised, which included two carboxyl functional groups. According to the literature, carboxyl is very easy to coordinate with metal ions (34, 35); thus, the gelation ability was tested by mixing ligand L17 and various metal salts with a 1:1 molar ratio in the component solvents such as MeOH–H<sub>2</sub>O (V/V = 1:1), heating to dissolve and then cooling to room temperature. L17 was found to form MOG at 1 wt% after 5 min in the presence of Ag(I). The gelation was confirmed by resistance to flow upon inversion of the screw-capped vials. Moreover, the individual L17 was not able to gelate in any solvent.

#### 3.2 Gelation behaviour of MOG in selected solvents

The gelation abilities of MOG were researched in a variety of polar, non-polar organic and component solvents (organic solvents–H<sub>2</sub>O (V/V = 1:1)), respectively. Gelation experiments with 1 wt% MOG in a selection of solvents were summarised in Table 1. As a result, MOG forms thermoreversible opaque gel within a few minutes in some polar solvents, such as DMF, MeOH and iPrOH. Firm gels were obtained not only from some pure solutions, such as MeOH, iPrOH and DMF, but also from some component solvents, such as MeOH–H<sub>2</sub>O (V/V = 1:1), EtOH–H<sub>2</sub>O (V/V = 1:1), iPrOH–H<sub>2</sub>O (V/V = 1:1), acetone–H<sub>2</sub>O (V/V = 1:1), acetonitrile–H<sub>2</sub>O (V/V = 1:1) and DMF–H<sub>2</sub>O (V/V = 1:1). It may be suggested that van der Waals interactions between the alkyl chains of gelator and solvent molecules were crucial for the self-assembly process required for gelation (38, 39). However, gelatin cannot be observed in non-polar solvents such as dichloromethane, chloroform and carbon tetrachloride. These results indicate that the polarity of the solvents has a significant effect on the formation of the gel.

In order to investigate the gelating abilities of MOG, minimum gelator concentration (MGC) values (Table 1), which is defined as the minimum amount of gelator required to gelate a given volume of solvent, have been determined for MOG. The thermal stability of the MOG was researched by measuring the gel–sol transition temperature (T<sub>gel</sub>). It was determined by heating the

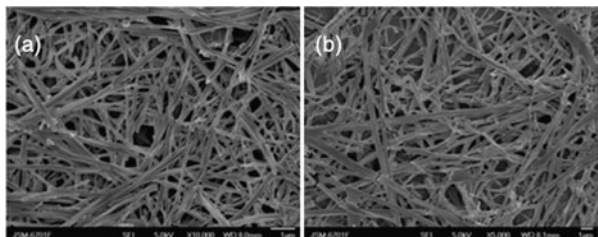


Figure 1. FESEM micrographs of the MOG. (a) MOG; (b) Xerogel of MOG on the glass sheet.

sample vial in the temperature-controlled water bath until tube inversion showed that the gel had melted. The higher thermal stability of the MOG in different solvents is shown by the high  $T_{\text{gel}}$  values (Table 1) and can be attributed to the stronger hydrogen bonding interaction among gelator molecules (40). The time of gel formation was also tested (Table 1).

Morphological features of the MOG have been studied using a FESEM. Figure 1 shows the FESEM image of the MOG in the presence of  $\text{AgNO}_3$ . It can be clearly seen that MOG forms nanofibrillar network structures from the FESEM, which might be responsible for encapsulating a large volume of solutions to form gels (Figure 1(a)). However, when the gel was dried onto the glass sheet, the FESEM image showed a discrete nanofibrillar network structures (Figure 1(b)). We proposed that the reason was the coordination ability of L17 and  $\text{Ag}^+$  became weaker when the gel was dried. As a result, L17 was self-assembled in the presence of selective valence metal ion  $\text{Ag}^+$  to form a nanofibrillar network structure that enables the trapping of a large volume of molecule containing solutions to form MOG. It may be suggested that metal ion chelation, intermolecular hydrogen bonding and  $\pi$ - $\pi$  stacking play a significant role in promoting the self-organisation and self-association of the L17 in the gel state.

To confirm whether cross-linking of gel fibres via metal coordination could have a significant strengthening effect, we compared the FT-IR spectra of the free L17 with its xerogel (Figure 2). The FT-IR spectra for xerogel of L17 showed distinct and interesting changes relative to the free L17. The strong absorption peaks at 1726.29 and  $1211.29\text{ cm}^{-1}$  can be assigned to combined C=O and C-O stretching vibrations, indicating the presence of protonated carboxylic acids. A strong absorption peak at  $1670.67\text{ cm}^{-1}$ , which is the characteristic of deprotonated carboxylic acids, was observed for free L17 (Figure 2(a)). The peak at  $1726.29\text{ cm}^{-1}$  corresponding to the carbonyl groups of free L17 decreased significantly in magnitude after an increase in  $\text{AgNO}_3$  content (Figure 2(b)). In addition, the C=O band shifted to lower wavenumbers when carboxyl groups coordinate with silver, from 1726.29 to  $1719.14\text{ cm}^{-1}$ . On the other hand, after an

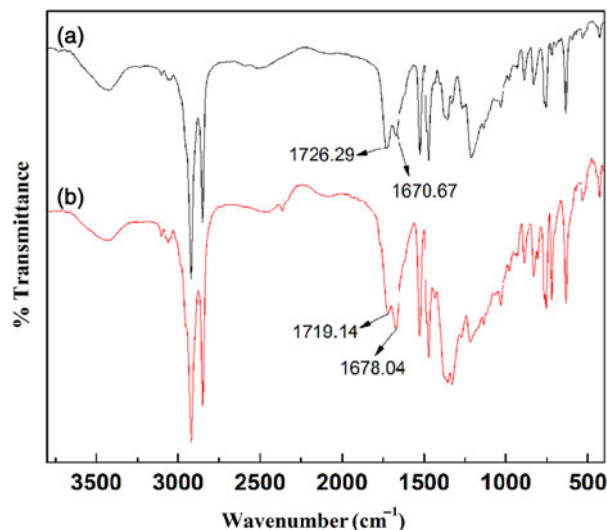


Figure 2. FTIR spectra of (a) L17 and (b) xerogel.

increase in  $\text{AgNO}_3$  content, the peak at  $1670.67\text{ cm}^{-1}$  corresponding to the carbonyl groups of free L17 increased significantly in magnitude (Figure 2(b)). Besides, the C=O band shifted to higher wavenumbers, from  $1670.67$  to  $1678.04\text{ cm}^{-1}$ . These changes suggest that silver ions had coordination with the carbonyl oxygen atom of protonated carboxyl functional groups and oxygen anion of deprotonated carboxyl functional groups of L17, respectively. These IR data suggest that  $\text{Ag(I)}$  has a very different effect on the L17. It also suggests that silver ion coordinated with the carboxyl groups of L17 induced the gel formation.

In order to establish the formation mechanism of xerogel, the XRD of L17 and MOG was determined (Figure 3). Compared with the L17, a sharp diffraction peak was obtained in the big angle region at  $2\theta = 39.7^\circ$ , which corresponds to a  $d$ -spacing of  $2.27\text{ \AA}$ , indicating the bond length of  $\text{Ag(I)}$  and carbonyl oxygen atom of

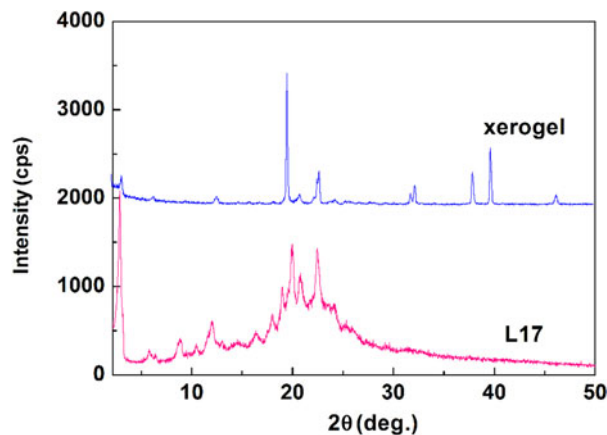


Figure 3. XRD diagram of L17 and xerogel.

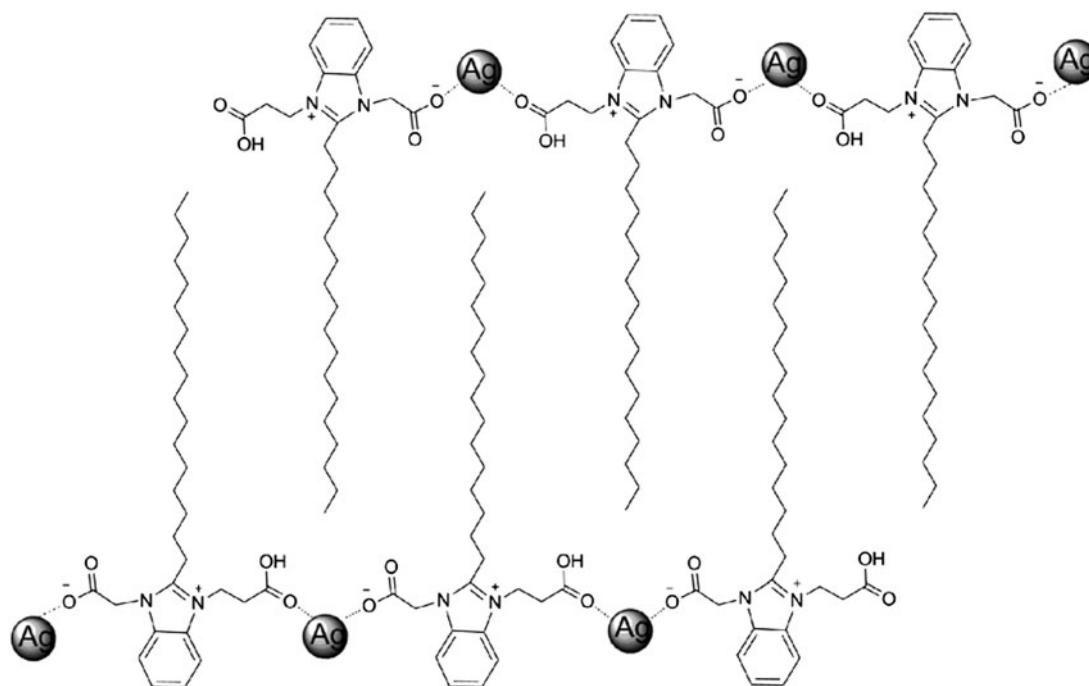


Figure 4. Schematic representation of the possible arrangement of molecules during MOG.

protonated carboxyl functional groups, and  $2\theta = 37.9^\circ$  which corresponds to a  $d$ -spacing of  $2.38 \text{ \AA}$  showing the bond length of Ag(I) and oxygen anion of deprotonated carboxyl functional groups (41, 42). The  $2\theta = 32.1^\circ$  corresponds to a  $d$ -spacing of  $2.79 \text{ \AA}$ , signifying the hydrogen bonding between unprotonated carboxyl functional groups and others; we also obtained a  $d$ -spacing of  $3.92 \text{ \AA}$  by  $2\theta = 22.7^\circ$ , which suggested that it was a  $\pi$ - $\pi$  stacking between aromatic nucleus (38). Besides, the  $2\theta = 19.5^\circ$  corresponds to a  $d$ -spacing of  $4.56 \text{ \AA}$ , expressing the van der Waals interactions between the long alkyl chains.

Thus, on the basis of the above spectroscopy, microscopic studies as well as the XRD results, it can be concluded that in the gelation process the MOG possibly forms repeating bilayers in which the molecules are connected by intermolecular hydrogen bonding and  $\pi$ - $\pi$  stacking (43). The possible interdigitated bilayer packing of the MOG is described in Figure 4. It has been shown that 1:1 complexes of L17 and silver ion can be prepared. The results of ESI-MS (calculated for  $(L17 + Ag^+ + 4H_2O)$  665.8 and found 665.6) experiments also support this hypothesis.

### 3.3 Sol-gel transformations of MOG by chemical stimuli

The transformation of gel-sol-gel has been observed by the addition of reasonable chemicals. For instance, the

addition of a few drops of  $NH_4OH$  to MOG resulted in clear colourless solutions (Figure 5). This transformation could be the result of the formation of the metal ammonia complex breaking the metal-ligand (L) coordination, which resulted in the clear solutions. The above result indicated that we should study the effect of the metal trapping reagent to trap the metal atoms in gel matrixes. In view of that purpose, we chose a well-known chelating agent EDTA. The same equivalents of EDTA were added to the gel as the equivalents of the metal salt in the gel. The vial was sealed and placed at room temperature. For MOG, which contains Ag(I) metal, the solid EDTA was found to penetrate slowly into the gel and thereby gradually transfer the gel into sol from top to bottom. About two days later, the whole gel turns into a clear transparent solution with a white coloured precipitate at the bottom of the vial. Our investigations present that the white coloured precipitate is an EDTA and L complex of Ag(I), while the clear solution

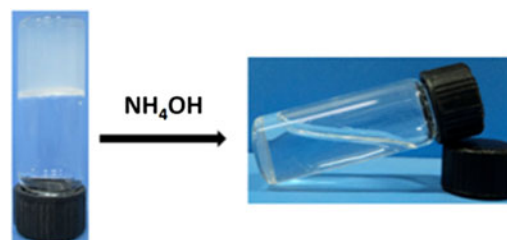


Figure 5. Illustration for gel-sol transformation of MOG by the addition of external chemical stimuli (ammonia).

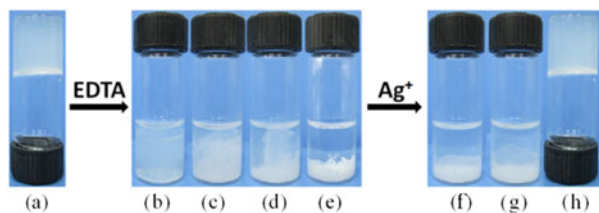


Figure 6. Illustration for reversible gel–sol transformation of MOG by the addition of EDTA and  $\text{AgNO}_3$ , respectively. (a) The 1:1 gel formed at 0.4 wt%; (b) immediately after addition of solid EDTA (1 equiv.); (c) after 1 h; (d) after 5 h; (e) after 12 h; (f) immediately after addition of  $\text{AgNO}_3$  (1 equiv.) to the above obtained solution; (g) after 30 min; (h) the ‘stable-to-inversion test’ succeeds after ultrasound.

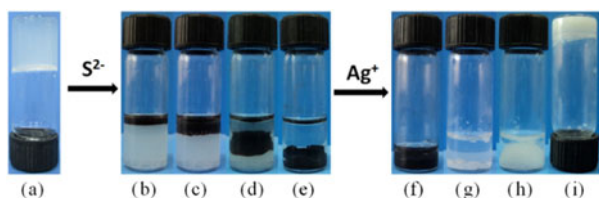


Figure 7. Illustration for reversible gel–sol transformation of MOG by the addition of  $\text{Na}_2\text{S}$  and  $\text{AgNO}_3$ , respectively. (a) The 1:1 gel formed at 0.4 wt%; (b) immediately after addition of solid  $\text{Na}_2\text{S}$  (1 equiv.); (c) after 4 min; (d) after 30 min; (e) after 12 h; (f)  $\text{Ag}_2\text{S}$  precipitate from (e); (g) immediately after addition of  $\text{AgNO}_3$  (1 equiv.) to the above obtained solution; (g) after 2 h; (h) after 6 h; (i) the ‘stable-to-inversion test’ succeeds.

is the acetonitrile– $\text{H}_2\text{O}$  ( $V/V = 1:1$ ) solution of the remaining ligand. Moreover, if we added  $\text{AgNO}_3$  into the clear solution again, it could be turned into a white coloured thick gel, similar to the beginning. It confirms that the colourless solution is the solution of the L (Figure 6). The same result could be observed if the same equivalents of  $\text{Na}_2\text{S}$  were added to the gel as the equivalents of the metal salt in the gel (Figure 7). Observably, the MOG responded to  $\text{Na}_2\text{S}$  rapidly. The gel surface immediately changed from white to colourless when it was exposed to  $\text{Na}_2\text{S}$ . After several hours of exposure, the MOG completely transformed into a

transparent sol, and the sol could transform into a gel again if we added silver ion to the solution after the black precipitate has been filtered off. The change from a gel to a sol could be evidently confirmed by SEM measurement. In the beginning stage of the complex gel being exposed to the  $\text{Na}_2\text{S}$ , we could see that the long and entangled belt-like fibres rapidly break into short and untangled fibrils (Figure 8(a)). Because the short belt-like fibres cannot keep the 3D network structure, which is crucial for the gel, the gel–sol transformation takes place. Substantially, the gel–sol transformation is evidently derived from the reaction of the  $\text{S}^{2-}$  with silver ion, which relieves the coordination of silver ion with L17 and thus destroys the gel structure. This was confirmed by the dark precipitate of silver sulphide after a longer time of exposure. If we add excess silver ion to the fluid solution again after the precipitate has been filtrated off, the gel re-forms (Figure 8(b)).

The pH responsiveness of the MOG was also investigated. This MOG showed a quick gel–sol transition upon addition of either base or acid (Figure 9). Added  $\text{HClO}_4$  (1 mol/l) to the 1:1 gel (1 wt%) at ambient temperature resulted in a gradual decomposition of the gelatinous state in about 10 min. Finally, we obtained a colourless, transparent solution (Figure 9(a)). Probably, this was due to carboxyl group protonation, causing breakage of the L17–Ag complexation and physical cross-linking. After stoichiometric addition of  $\text{NaOH}$  (1 mol/l) to the solution obtained from the  $\text{HClO}_4$  disintegrated MOG, the stable sol state was completely converted into a gel after sonication for a few seconds. However, by adding  $\text{NaOH}$  (1 mol/l) to the 1:1 gel, small amount of white colour precipitate was observed in the sol state (Figure 9(c)). We attributed this to the formation of silver hydroxide, resulting in a transformation from the gel to sol. After stoichiometric addition of  $\text{HClO}_4$  (1 mol/l) to this solution followed by sonication for a few seconds, the solution turned back to gel rapidly. These pH-dependent gel–sol transformations came from the reversible protonation reactions of the carboxyl groups. The pH cycling experiments showed that the process was repeated at least

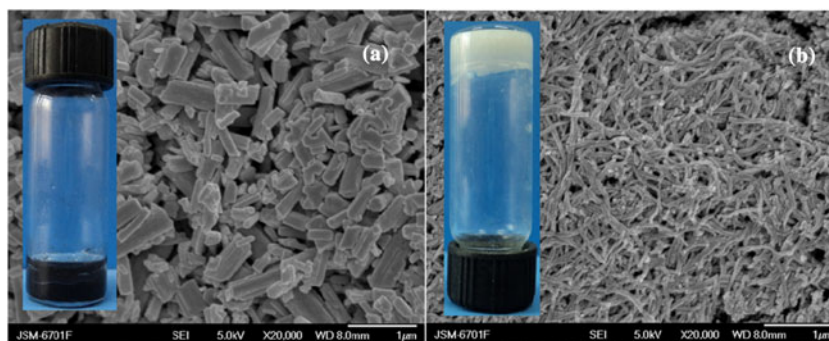


Figure 8. SEM images corresponding to the  $\text{Ag}_2\text{S}$  precipitate in (a) and the reform gel (b), respectively.

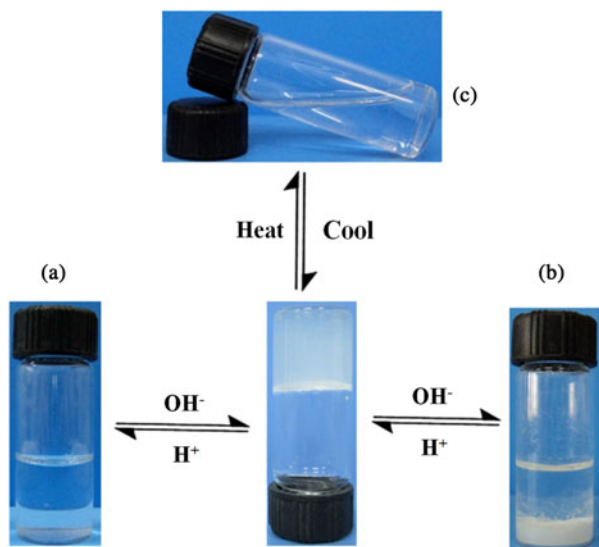


Figure 9. Illustration for pH reversibility and thermoreversibility of MOG.

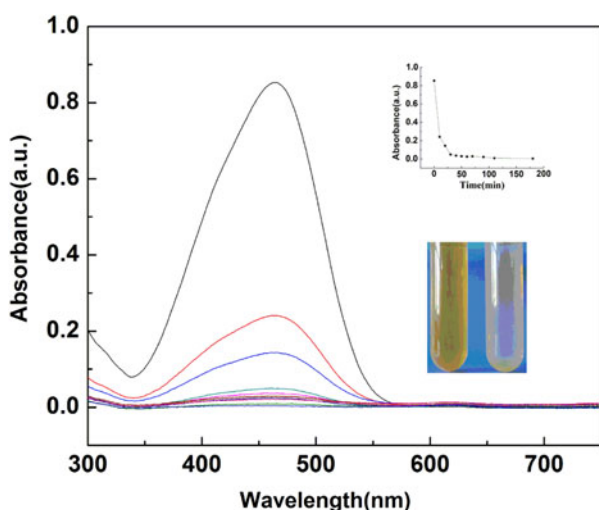


Figure 10. UV-vis spectra of dye solution (black line) after the addition of MOG xerogel at various time intervals (colored lines).

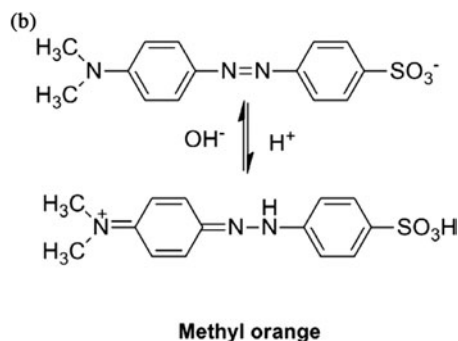
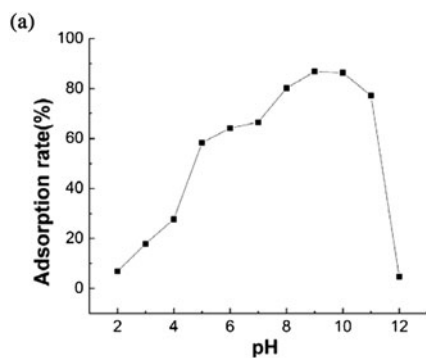


Figure 11. (a) Dye adsorption onto MOG as a function of pH. (b) Structure of methyl orange at different pH.

two times. Besides, when the temperature reached a limit of 80°C, the gelation of a 1:1 gel was observed in all heating-cooling cycles, suggesting the thermoreversibility of the MOG (Figure 9(b)).

### 3.4 Dye sorption by MOG

The elimination of toxic dye substances from wastewater has been a major concern. There are several types of smart materials, such as clays, dendritic polymers and supramolecular gels, which were shown to act as efficient dye sorbent in the literature (44, 45). Universally, the dye sorbent should include two domains: hydrophilic domain to interact with water and hydrophobic domain to absorb the dye. The ligand L17 possesses both features, so the MOG of L17 may have a potential to act as a dye sorbent. For this purpose, xerogel of the MOG was tested for methyl orange dye sorption. A total of 6 mg of methyl orange dye was dissolved in 500 ml of distilled water to prepare the stock solution of dye. In a typical reaction, 5 mg of xerogel was immersed in 7 ml of the above solution in a vial and left undisturbed for 3 h. After 3 h, it was shown that almost the whole dye was transferred from aqueous solution to xerogel, resulting in an almost clear water solution in the vial. At various time intervals during 3 h, the sorption of dye from aqueous solution by xerogel was detected by UV-visible spectra (Figure 10).

In order to understand the sorption mechanism clearly, the sorption capacity of sorbent that was affected by the pH change in the solution has been investigated (Figure 11(a)). It is well known that methyl orange can exist in both anionic form at basic pH and cationic form at acidic pH (Figure 11(b)), and the benzimidazolium in MOG is positively charged, so the initial pH of the dye solution plays a significant role in the sorption process. Lower sorption at  $\text{pH} < 4$  is due to the interionic repulsion between the positively charged dye molecule and the sorbent. At  $\text{pH} > 4$ , the methyl orange molecules were deprotonated, which results in an electrostatic attraction between negatively charged dye molecule,

positively charged sorbent and silver ions to the maximum removal. As pH increased from 11 to 12, the formation of silver hydroxide resulted in the collapse of the 3D network. It indicates that the electrostatic mechanism is not the sole mechanism for dye sorption, in that the 3D networks are also responsible for sorption. We had also researched the sorption of gel for methyl orange dye, the result indicated that gel has weak sorption capacity as compared with xerogel in a same time. It must be that there are a large number of solution molecules in the nanofibrillar network structures, so it will decrease the sorption capacity of gel for methyl orange.

#### 4. Conclusions

The gelating properties of L17 ligand in the presence of transition metal salt ( $\text{AgNO}_3$ ) have been thoroughly investigated. It was suggested that the coordination of metal to ligand plays a key role in the formation of MOG. Compared with previous literature about stimuli responsive of MOG, it was found to be a multi-responsiveness supramolecular MOG and showed good stimuli responsiveness towards the changes in pH, EDTA,  $\text{Na}_2\text{S}$  and  $\text{NH}_3$  solutions. These results proved the importance of the coordination bond in the gelation process. We can also use the xerogel for the methyl orange dye sorption and then obtain a desired result. Finally, the application of the gel in sewage purification, which contains some dye molecules, becomes possible.

#### Acknowledgements

This work was supported by the National Natural Science Foundation of China (Nos 21064006, 21262032 and 21161018), the Program for Changjiang Scholars and Innovative Research Team in University of Ministry of Education of China (No. IRT1177), the Natural Science Foundation of Gansu Province (No. 1010RJZA018), the Youth Foundation of Gansu Province (No. 2011GS04735) and NWNNU-LKQN-11-32.

#### References

- (1) Adalar, T.K.; Adarsh, N.N.; Sankolli, R.; Dasti dar, P. *Beilstein J. Org. Chem.* **2010**, *6*, 848–858.
- (2) Zhou, G.R.; Li, Y.J.; Yu, X.D.; Yu, D.C.; Yin, Y.B. *Supramol. Chem.* **2012**, *24*, 234–237.
- (3) Jin, Q.X.; Zhang, L.; Zhu, X.F.; Duan, P.F.; Liu, M.H. *Chem. Eur. J.* **2012**, *18*, 4916–4922.
- (4) Gong, R.Y.; Song, Y.B.; Guo, Z.X.; Li, M.; Jiang, Y.; Wan, X.B. *Supramol. Chem.* **2013**, *25*, 269–275.
- (5) Kim, J.; Singh, N.; Lyon, L.A. *Angew. Chem., Int. Ed.* **2006**, *45*, 1446–1449.
- (6) Kurisawa, M.; Chung, J.E.; Yang, Y.Y.; Gao, J.S.; Uyama, H. *Chem. Commun.* **2005**, 4312–4314.
- (7) Kiyonaka, S.; Sugiyaou, K.; Shinkai, S.; Hamachi, I. *J. Am. Chem. Soc.* **2002**, *124* (37), 10954–10955.
- (8) Bhuniya, S.; Park, S.M.; Kim, B.H. *Org. Lett.* **2005**, *7*, 1741–1744.
- (9) Chen, L.Q.; Wu, J.C.; Yuwen, L.H.; Shu, T.M.; Xu, M.; Zhang, M.M.; Yi, T. *Langmuir.* **2009**, *25*, 8434–8438.
- (10) Shi, J.f.; Gao, Y.; Yang, Z.M.; Xu, B. *Beilstein J. Org. Chem.* **2011**, *7*, 167–172.
- (11) Maitra, U.; Chakrabarty, A. *Beilstein J. Org. Chem.* **2011**, *7*, 304–309.
- (12) Weng, W.G.; Benjamin Beck, J.; Jamieson, A.M.; Rowan, S.J. *J. Am. Chem. Soc.* **2006**, *128*, 11663–11672.
- (13) Samai, S.; Biradha, K. *Chem. Mater.* **2012**, *24*, 1165–1173.
- (14) George, M.; Funkhouser, G.P.; Weiss, R.G. *Langmuir.* **2008**, *24*, 3537–3544.
- (15) Wu, J.C.; Yi, T.; Shu, T.M.; Yu, M.X.; Zhou, Z.G.; Xu, M.; Zhou, Y.F.; Zhang, H.J.; Han, J.T.; Li, F.Y.; Huang, C.H. *Angew. Chem., Int. Ed.* **2008**, *47*, 1063–1067.
- (16) Wu, J.C.; Yi, T.; Xia, Q.; Zou, Y.; Liu, F.; Dong, Jie; Shu, T.M.; Li, F.Y.; Huang, C.H. *Chem. Eur. J.* **2009**, *15*, 6234–6243.
- (17) Yu, X.D.; Liu, Q.; Wu, J.C.; Zhang, M.M.; Cao, X.H.; Zhang, S.; Wang, Q.; Chen, L.M.; Yi, T. *Chem. Eur. J.* **2010**, *16*, 9099–9106.
- (18) Yu, X.D.; Cao, X.H.; Chen, L.M.; Lan, H.C.; Liu, B.; Yi, T. *Soft Matter.* **2012**, *8*, 3329–3334.
- (19) Hamilton, T.D.; Burćar, D.; Baltrusaitis, J.; Flanagan, D.R.; Li, Y.J.; Ghorai, S.; Tivanski, A.V.; MacGillivray, L.R. *J. Am. Chem. Soc.* **2011**, *133*, 3365–3371.
- (20) Naota, T.; Koori, H. *J. Am. Chem. Soc.* **2005**, *127*, 9324–9325.
- (21) Cravotto, G.; Cintas, P. *Chem. Soc. Rev.* **2009**, *38*, 2684–2697.
- (22) Kishimura, A.; Yamashita, T.; Aida, T. *J. Am. Chem. Soc.* **2005**, *127*, 179–183.
- (23) Kuroiwa, K.; Shibata, T.; Takada, A.; Nemoto, N.; Kimizuka, N. *J. Am. Chem. Soc.* **2004**, *126*, 2016–2021.
- (24) Piepenbrock, M.O.M.; Clarke, N.; Steed, J.W. *Soft Matter.* **2010**, *6*, 3541–3547.
- (25) Hou, J.; Wu, X.; Li, Y.J. *Supramol. Chem.* **2011**, *23*, 533–538.
- (26) Peng, F.; Li, G.Z.; Liu, X.X.; Wu, S.Z.; Tong, Z.H. *J. Am. Chem. Soc.* **2008**, *130*, 16166–16167.
- (27) Zhou, Y.F.; Xu, M.; Yi, T.; Xiao, S.Z.; Zhou, Z.G.; Li, F.Y.; Huang, C.H. *Langmuir.* **2007**, *23*, 202–208.
- (28) Komatsu, H.; Matsumoto, S.; Tamaru, S.; Kaneko, K.; Ikeda, M.; Hamachi, I. *J. Am. Chem. Soc.* **2009**, *131*, 5580–5585.
- (29) Zhang, S.; Yang, S.; Lan, J.; Yang, S.; You, J. *Chem. Commun.* **2008**, 6170–6172.
- (30) Sambri, L.; Cucinotta, F.; Paoli, G.D.; Stagni, S.; Cola, L.D. *New J. Chem.* **2010**, *34*, 2093–2096.
- (31) Piepenbrock, M.O.M.; Clarke, N.; Steed, J.W. *Soft Matter.* **2011**, *7*, 2412–2418.
- (32) Yang, L.; Luo, L.; Zhang, S.; Su, X.; Lan, J.; Chen, C.T.; You, J. *Chem. Commun.* **2010**, *46*, 3938–3940.
- (33) Ray, S.; Das, A.K.; Banerjee, A. *Chem. Mater.* **2007**, *19*, 1633–1639.
- (34) Zhang, Y.M.; Zhang, W.Q.; Li, J.Q.; Dang, J.P.; Wei, T.B. *Mater. Lett.* **2012**, *82*, 227–229.
- (35) Wei, T.B.; Dang, J.P.; Lin, Q.; Yao, H.; Liu, Y.; Zang, Y.M. *Sci. China Chem.* **2012**, *55*, 2471–2626.
- (36) Zhang, Y.M.; Lin, Q.; Wei, T.B.; Qin, X.P.; Li, Y. *Chem. Commun.* **2009**, 6074–6076.
- (37) Pool, W.O.; Harwood, H.J.; Ralston, A.W. *J. Am. Chem. Soc.* **1937**, *59*, 178–179.

- (38) Tu, T.; Assenmacher, W.; Peterlik, H.; Schnakenburg, G.; Heinz Dötz, K. *Angew. Chem., Int. Ed.* **2008**, *47*, 7127–7131.
- (39) Lu, C.C.; Su, S.K. *Supramol. Chem.* **2009**, *21*, 572–580.
- (40) Suman, S.; Joykrishna, D.; Kumar, B. *Soft Matter* **2011**, *7*, 2121–2126.
- (41) Rasika Dias, H.V.; Polach, S.A. *Inorg. Chem.* **2000**, *39*, 4676–4677.
- (42) Erxleben, A. *Inorg. Chem.* **2001**, *40*, 2928–2931.
- (43) Brahmachari, S.; Debnath, S.; Dutta, S.; Kumar Das, P. *Beilstein J. Org. Chem.* **2010**, *6*, 859–868.
- (44) Sayari, A.; Hamoudi, S.; Yang, Y. *Chem. Mater.* **2005**, *17*, 212–216.
- (45) Tu, T.; Bao, X.L.; Assenmacher, W.; Peterlik, H.; Daniels, J.; Dötz, K.H. *Chem. Eur. J.* **2009**, *15*, 1853–1861.